Electric Field Effects on Barium Autoionizing Spectra

Darrell J. Armstrong, Chris H. Greene, Robert P. Wood, and J. Cooper

Joint Institute for Laboratory Astrophysics and Department of Physics, University of Colorado, Boulder, Colorado 80309-0440

(Received 30 November 1992)

Stark spectra for atomic barium in the autoionizing region below the $5d_{3/2}$ ionization threshold are studied by photoionization of the laser-excited $5d6p\ ^3D^0_1$ bound level, in a combined experimental and theoretical study. The electric field dramatically increases the complexity of the resonance pattern beyond that of the already complex zero-field spectrum. A quantum defect and R-matrix calculation describes 86 relevant zero-field channels. A frame transformation couples these channels together nonperturbatively in the presence of the field, reproducing most of the observations.

PACS numbers: 32.80.Fb, 32.80.Dz, 32.80.Rm

Dielectronic recombination (DR) cross sections are now known to be unusually sensitive to an external electric field, following a theoretical prediction by Jacobs, Davis, and Kepple [1] that was verified experimentally by Belic *et al.* [2]. While this showed the qualitative effect of a strong electric field, it has become increasingly apparent that our theoretical understanding of atomic autoionizing states in a static electric field is not yet adequate. Calculations [3] of field effects on DR cross sections have resorted to an oversimplified description of the autoionization dynamics. This Letter develops the first microscopically accurate theoretical description of doubly excited autoionizing states in an electric field. The accuracy of the resulting Stark effect calculation is demonstrated by comparing theory with new measurements of barium photoionization in the presence of a static electric field. This process amounts to the time reverse of a particular channel that operates when DR takes place in a field.

The properties of a two-electron atom in an electric field are also of fundamental interest because this system has a comparatively simple nonseparable Schrödinger equation that exhibits tremendous complexity. The number of Rydberg channels is even higher than in recent studies [4] of another fundamental nonseparable system: atomic lithium in a 6 T magnetic field.

Most Stark effect experiments have been carried out for the alkali metal atoms or hydrogen. Such "one-electron" atomic spectra in an electric field have been successfully handled by the local frame transformation theory of Fano [5] and Harmin [6]. Gallagher and co-workers [7] observed field effects on autoionizing levels of Ba in several energy ranges. König *et al.* [8] measured Stark spectra of Ba below the zero-field ionization threshold, and modeled them using the Harmin-Fano theory. Kelleher and co-workers [9] measured Ba autoionizing spectra in an electric field, and interpreted them using a semiempirical diagonalization method.

Field-free barium autoionizing spectra have been accurately described only recently by a series of nearly *ab initio* eigenchannel R-matrix calculations described in Ref. [10]. These calculations determine "smooth, short-range" scattering matrices and dipole photoabsorption amplitudes [in the usual sense of multichannel quantum defect theory (MQDT)], from which the zero-field atomic spectra can be easily obtained. These same scattering and dipole amplitudes serve as the input information needed for the Harmin-Fano [5,6] local frame transformation from spherical to parabolic coordinates. We show below how MQDT, in combination with the Harmin-Fano theory, can reliably predict Stark spectra of two-electron atoms above the zero-field ionization threshold despite the extraordinary number of interfering excitation and decay pathways.

The experimental Stark spectra shown in Figs. 1 and 2 were recorded by photoionizing barium atoms in a thermal atomic beam in the presence of dc electric fields of up to 9 kV/cm. Nd:YAG-pumped pulsed dye lasers with 5 ns pulse durations intersected the barium beam between field plates (one biased positive, the other negative) in high vacuum. The exciting laser was tuned into resonance with the $5d6p\ ^3D^0_1$ bound level at 413.4 nm, while

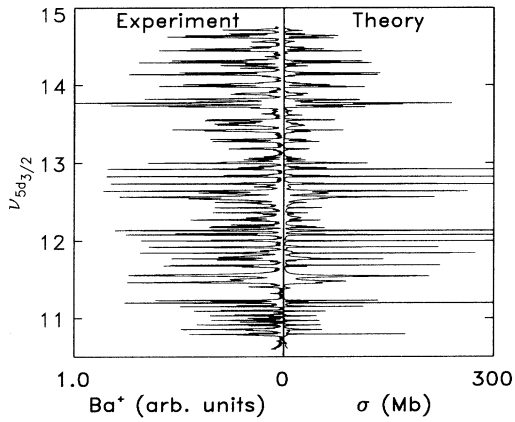

FIG. 1. Experimental (relative) and theoretically calculated photoionization spectrum of the barium $5d6p\ ^3D_1$ level at a field strength of 6 kV/cm. The horizontal axis represents the cross section while the vertical axis is an energy variable—the final state effective quantum number $\nu_{5d_{3/2}}$.

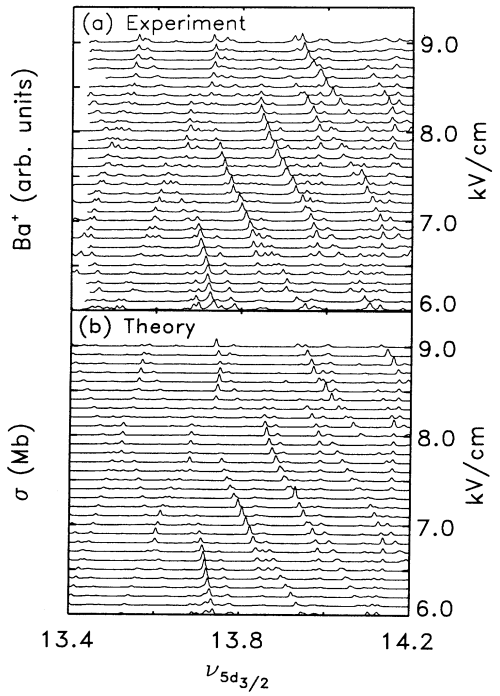

FIG. 2. Present relative experimental (a) and theoretical (b) Stark maps, showing cross section vs effective quantum number over a range of electric fields ranging from 6 kV/cm up to 9 kV/cm. In the theoretical map, the baselines for each successive field are separated by 400 Mb.

the ionizing laser was scanned across the autoionizing region below the $5d_{3/2}$ ionization threshold, from 460 to 450 nm. The positive and negative voltages on the field plates were adjusted so that barium ions were swept out of the beam and impinged on the first dynode of an electron multiplier with the same incident energy independent of the electric field strength. The multiplier signal went to a gated integrator and boxcar averager, whose output was digitized and stored. Absolute wavelength calibration was achieved by using either a monochromator, or when convenient, the position of a known zero-field resonance. The experimental methods (except for the addition of dc fields) are discussed further in a recent zero-field measurement of the $5d6p\ ^3D_1^0$ photoionization cross section [11].

All calculations presented in this paper use the "quasi-discrete" approximation [12], which neglects tunneling under the Coulomb-Stark barrier in the downfield parabolic coordinate. We further assume that in the autoionization range between the Ba^+ $6s$ and $5d$ thresholds treated here, the electric field does not affect the photoelectron escape probability when it moves in the continua associated with the open $6s$ channels. The escape of a photoelectron beyond a short-range reaction volume (whose radius is 20 a.u. for the present calculations) is described in zero field by a set of reaction matrices and dipole matrix elements. That is, the $F=0$ reaction-matrix solutions, initially calculated in a $(J_c,j)JM$ coupling scheme (I), have the structure

$$\Psi_{i'}=\mathcal{A}\sum_i \Phi_i (f_i(r)\delta_{ii'}-g_i(r)K_{ii'}^{(\mathrm{I})}) . \quad (1)$$

Here the index i labels different channels, i.e., $i\equiv\{N_c \times[(S_c,L_c)J_c,(sl)j]JM\}$. Here the principal quantum number of the residual ionic core state is N_c, while the core spin, orbital, and total angular momenta are S_c, L_c, and J_c, respectively. In the energy range considered here only the $6s_{1/2}$, $5d_{3/2}$, $5d_{5/2}$, $6p_{1/2}$, and $6p_{3/2}$ ionic states are relevant, and their interaction with the field is negligible. The photoelectron quantum numbers are similarly s,l,j. The reaction matrix is diagonal in the total angular momentum J and projection M quantum numbers. Moreover M remains conserved in the presence of the electric field, provided the angular momentum quantization axis z is chosen to lie along the field. The channel function Φ_i contains the dependence of the wave function on all spin and spatial coordinates of the system *except* the radial distance r of the outermost electron from the nucleus. (f_i,g_i) in Eq. (1) are regular and irregular radial Coulomb functions.

Electric field effects on the outermost atomic electron are simpler to describe in another representation where l,m of the outer electron appear explicitly. We use the channel index k to denote the zero-field channels in this uncoupled representation (II), i.e., $k\equiv\{N_c[(S_c,L_c)J_c,s] \times J_{cs}M_{cs},lm\}$. The quantum number J_{cs} is the result of combining the core total angular momentum with the photoelectron spin. A standard angular momentum recoupling matrix X_{ik} relates the solutions (I) to those (II) in the uncoupled J_{cs} scheme k. The reaction matrix $K^{(\mathrm{II})}$ in the new scheme is given in terms of the one $K^{(\mathrm{I})}$ in Eq. (1) by $K^{(\mathrm{II})}=\tilde{X}K^{(\mathrm{I})}X$, where $\tilde{X}$ denotes the transpose of X. The dipole matrix elements connecting an initial state to the K-matrix final states in the two different coupling schemes are related by $d^{(\mathrm{II})}=\tilde{X}d^{(\mathrm{I})}$. For notational brevity we will use the nonsuperscripted quantities K,d to denote the zero-field $K^{(\mathrm{II})},d^{(\mathrm{II})}$.

The experimental results reported here all involve laser excitation of the Ba $5d6p\ ^3D_1^0$ state, followed by its photoionization with a second laser whose wavelength is scanned. Both lasers are linearly polarized along the field axis, whereby only $M=0$ final states are relevant (ignoring hyperfine depolarization effects, which are discussed elsewhere [11]). In the absence of an electric field, only the final state symmetries $J^\pi=0^+,2^+$ would contribute, and in representation I these are the only symmetries having nonzero dipole matrix elements. The electric field, however, couples these two final state symmetries to numerous other symmetries. If we restrict our attention to $6s\epsilon l$ channels having $l\leq 4$, to $5d\epsilon l$ channels having $l\leq 3$, and to $6p\epsilon l$ channels having $l\leq 1$, a total of 86 $M=0$ channels are relevant. The values of J^π followed by the number of channels in parentheses are

$$\{0^+(5),1^+(11),2^+(11),3^+(8),4^+(5),5^+(2),0^-(4),1^-(10),2^-(11),3^-(9),4^-(6),5^-(3),6^-(1)\},$$

giving the total number of 86 channels. Each of these 11 symmetries listed requires a separate eigenchannel R-matrix calculation of the type discussed in [10] to determine the zero-field K,d. The reaction and dipole matrix elements for all higher partial waves and associated symmetries are assumed to vanish, a reasonable approximation for sufficiently large field strengths in the range treated here. For very small field strengths in the V/cm range, relevant to dielectronic recombination measurements [2], the small nonzero quantum defects of higher partial waves must be included.

At this point we use the standard matrix manipulations of MQDT to impose large-r boundary conditions in the energetically open (o) and "closed" (c) channels. This determines the "physical K matrix" of conventional scattering theory, whose indices include physically open channels only. For the present calculations these are the channels attached to the $6s$ threshold of Ba^+ only. In a partitioned matrix notation frequency used in MQDT, this K matrix is

$$K^{\text{phys}}=K^{oo}-K^{oc}(K^{cc}+W^{cc})^{-1}K^{co}, \tag{2}$$

while the corresponding dipole matrix elements to the physical K matrix states are obtained from

$$d^{\text{phys}}=d^{o}-K^{oc}(K^{cc}+W^{cc})^{-1}d^{c}. \tag{3}$$

Finally the total photoionization cross section is $\sigma \propto \omega \tilde{d}^{\text{phys}}[I+(K^{\text{phys}})^2]^{-1}d^{\text{phys}}$, with ω the frequency of the ionizing photon.

The remaining quantity to be defined in these expressions is the matrix W^{cc} having closed channel indices only. In zero field, this matrix is simply a diagonal matrix with elements $W^{cc}_{kk'}=\tan(\pi\nu_k)\delta_{kk'}$, where ν_k is the effective quantum number in closed channel k. For a nonzero field F, the photoionization cross section is calculated using these same formulas. In place of the preceding expression for W^{cc}, however, one must use the field-dependent quantity:

$$W_{kk'}=\delta_{N_c,N_c'}\delta_{L_c,L_c'}\delta_{J_c,J_c'}\delta_{J_{cs},J_{cs}'}\delta_{M_{cs},M_{cs}'}\delta_{mm'}(-h_F^{(m)})^{-1}_{l,l'}. \tag{4}$$

The matrix $(h_F^{(m)})_{l,l'}$, is precisely the real, symmetric hydrogen Stark matrix for which Harmin uses the same notation in [6]. Harmin calculates this quantity as $(-h_F)^{-1}=U^{-1}\tan\phi\tilde{U}^{-1}$, in terms of the parabolic-spherical transformation matrix $U^{(m)}_{\beta,l}$ and the inner-well WKB phase ϕ_β in the "downfield" parabolic coordinate η for a hydrogenic Stark state β. (Our neglect of Stark tunneling ionization amounts to neglecting Harmin's Stark amplitude matrix H_F, as in [12].) The full matrix $W_{kk'}$ can be viewed qualitatively as an "outer-field" reaction matrix for scattering of an electron of orbital momentum $l_{k'}$ into orbital momentum l_k when it is reflected by the Coulomb-Stark potential barrier formed at large distances. Tunneling through the barrier is possible in principle. However, since WKB tunneling amplitudes are exponentially small (except near the top of a barrier), we neglect tunneling totally in this paper. The states we are treating have another more likely decay route to the continuum, namely, energy exchange between the Rydberg electron and the Ba^+ electron(s).

The theoretical spectra shown in this paper have been convolved with the 0.5 cm^{-1} experimental linewidth. Figure 1 compares as a mirror image the experimental and calculated spectra of a field strength of 6 kV/cm, over a broad energy range from below the Inglis-Teller limit (occurring at $\nu=12.3$ for this field) up to energies well above this limit. This limit is where different Stark n manifolds begin to overlap in hydrogen. One sees at low energies the hydrogenic high-l manifold centered on integer values of the effective quantum number $\nu_{d_{3/2}}$ relative to the $Ba^+(5d_{3/2})$ threshold, while for higher energies the spectrum becomes substantially more complicated owing to the numerous overlapping and mutually perturbing levels. This pattern, in which high-l hydrogenic manifolds fan out and acquire the autoionization width of the lower-l states, is a characteristic feature that occurs in the Stark spectra of all autoionizing atoms and molecules. Generally good agreement is found between the experimental and theoretical features, particularly in view of the striking complexity of the spectra. The intensities of many narrow lines are consistently underestimated by theory, which is most noticeable in the high-l hydrogenic Stark manifolds below the Inglis-Teller (n-mixing) limit. This may derive in part from an energy mesh that is not dense enough to represent the narrowest features in Fig. 1, even though the MQDT calculation was performed at 20000 energy mesh points prior to convolution with the experimental resolution. Also, occasional isolated lines are present in the experiment that have no theoretical counterpart. Many are caused by a breakdown of the electronic selection rule for exciting only $M=0$ final states in the 18% of natural barium isotopes having nonzero nuclear spin. This breakdown is documented in detail elsewhere [11] for the zero-field barium spectrum.

As a second example, Fig. 2 compares the experimental and theoretical Stark maps over a smaller energy range covering electric fields from 6 to 9 kV/cm . Such maps show the continuity of resonances evolving from one field strength to the next. Some intriguing features in Fig. 2 are avoided crossings between autoionizing resonances that frequently exchange the resonance characteristics such as the width and strength. One example is the intense resonance centered near $\nu_{d_{3/2}}=13.7$ at 6.2 kV/cm. As the field is increased the resonance strength shows little change initially, but at 7.0 kV/cm and higher fields it has abruptly "disappeared." Other similar examples can

be identified. Such features are characteristic of all parameter-dependent Rydberg spectra in real atoms and molecules [4,13]. The residual discrepancies between theory and experiment appear to be caused by small errors in the zero-field reaction matrices whose effects are especially important when resonance pathways interfere sensitively.

The experimental Stark measurements presented here, along with the accompanying calculations, provide detailed evidence confirming that a quantitative description of autoionizing states of many-electron atoms in an electric field is now possible. The complexity of the barium Stark spectrum is evident from the fact that the calculations show roughly 600 $M=0$ autoionizing resonances in the ≈ 500 cm^{-1} energy range covered in Fig. 1. (Only half of these are observable in this polarization scheme owing to reflection symmetry through any plane containing the field axis.) Extension of the present theoretical approach to include tunneling effects and the interference "ripples" near each ionization threshold appears to be straightforward, following Refs. [6]. This would pose difficulties, however, for methods based on matrix diagonalization, such as Ref. [9], or for perturbative methods.

From the formulas presented above and from the expressions for h_F given in Refs. [6,12], the present calculations are relatively straightforward once the zero-field quantities K,d are known. (These have been determined by methods discussed in [10] and are available from the authors upon request, and will be discussed in a subsequent publication.) While the Stark effect of one-electron excited states has been understood for some time [6,12] and zero-field spectra of doubly excited atoms more recently [10], this work has shown that nonperturbative field effects on two-electron atoms can now be described with similar accuracy. This opens the door to a quantitatively correct description of field effects on dielectronic recombination.

This work was supported in part by the National Science Foundation. Discussions with D. Harmin and T. Bergeman have been helpful. Access to the laboratory of S. Smith is gratefully acknowledged.

[1] V. L. Jacobs, J. Davis, and P. C. Kepple, Phys. Rev. Lett. **37**, 1390 (1976); V. L. Jacobs and J. Davis, Phys. Rev. A **19**, 776 (1979).

[2] D. S. Belic, G. H. Dunn, T. J. Morgan, D. W. Mueller, and C. Timmer, Phys. Rev. Lett. **50**, 339 (1983).

[3] K. LaGattuta and Y. Hahn, Phys. Rev. Lett. **51**, 558 (1983).

[4] C. Iu, G. R. Welch, M. M. Kash, D. Kleppner, D. Delande, and J. C. Gay, Phys. Rev. Lett. **66**, 145 (1991); P. F. O'Mahony and F. Mota-Furtado, *ibid.* **67**, 2283 (1991); S. Watanabe and H. Komine, *ibid.* **67**, 3227 (1991).

[5] U. Fano, Phys. Rev. A **24**, 619 (1981).

[6] D. A. Harmin, in *Atoms in Strong Fields*, edited by C. A. Nicolaides, C. W. Clark, and M. H. Nayfeh (Plenum, New York, 1990), p. 61, and references therein; Phys. Rev. A **26**, 2656 (1982).

[7] K. A. Safinya, J. F. Delpech, and T. F. Gallagher, Phys. Rev. A **22**, 1062 (1980); W. Sandner, K. A. Safinya, and T. F. Gallagher, *ibid.*, **24**, 1647 (1981); S. M. Jaffe, R. Kachru, N. H. Tran, H. B. van Linden van den Heuvell, and T. F. Gallagher, *ibid.* **30**, 1828 (1984); R. R. Jones and T. F. Gallagher, *ibid.* **39**, 4583 (1989).

[8] A. König, J. Neukammer, H. Hieronymus, and H. Rinneberg, Phys. Rev. A **43**, 2402 (1991).

[9] D. E. Kelleher and E. B. Saloman, Phys. Rev. A **35**, 3327 (1987); E. B. Saloman, J. W. Cooper, and D. E. Kelleher, Phys. Rev. Lett. **55**, 193 (1985).

[10] C. H. Greene and M. Aymar, Phys. Rev. A **44**, 1773 (1991), and references therein.

[11] D. J. Armstrong, R. P. Wood, and C. H. Greene, Phys. Rev. A **47**, 1981 (1993); see also R. P. Wood, C. H. Greene, and D. Armstrong, Phys. Rev. A **47**, 229 (1993).

[12] D. A. Harmin, Phys. Rev. A **30**, 2413 (1984); K. Sakimoto, J. Phys. B **22**, 2727 (1989).

[13] P. Gaspard, S. A. Rice, and K. Nakamura, Phys. Rev. Lett. **63**, 930 (1989); Q. Wang and C. H. Greene, Phys. Rev. A **44**, 1874 (1991).